ACS APPLIED MATERIALS & INTERFACES

Research Article

www.acsami.org

Fabrication and Characterization of Plasma-Polymerized Poly(ethylene glycol) Film with Superior Biocompatibility

Changrok Choi,[†,▽] Inseong Hwang,[‡,▽] Young-Lai Cho,[†] Sang Y. Han,[†] Dong H. Jo,[§] Donggeun Jung,[∥] Dae W. Moon,[†,⊥] Eun J. Kim,[‡] Chang S. Jeon,[‡] Jeong H. Kim,*[,§,#] Taek D. Chung,*[,‡] and Tae G. Lee*[,†,⊥]

[†]Center for Nano-Bio Convergence, World Class Laboratory, Korea Research Institute of Standards and Science, Daejeon, 305-340, Korea

[‡]Department of Chemistry, College of Natural Science, Seoul National University, Seoul 151-742, Korea

[§]Fight against Angiogenesis-Related Blindness (FARB) Laboratory, Clinical Research Institute, Seoul National University Hospital & Department of Ophthalmology, College of Medicine, Seoul National University, Seoul 110-744, Korea

[∥]Department of Physics, Sungkyunkwan University, Suwon, 440-746, Korea

[⊥]Department of Nano and Bio Surface Science, University of Science and Technology, Daejeon, 305-340, Korea

[#]Tumor Microenvironment Research Center, Global Core Research Center, Seoul National University, Seoul 151-742, Korea

Supporting Information

ABSTRACT: A newly fabricated plasma-polymerized poly(ethylene glycol) (PP-PEG) film shows extremely low toxicity, low fouling, good durability, and chemical similarity to typical PEG polymers, enabling live cell patterning as well as various bioapplications using bioincompatible materials. The PP-PEG film can be overlaid on any materials via the capacitively coupled plasma chemical vapor deposition (CCP-CVD) method using nontoxic PEG200 as a precursor. The biocompatibility of the PP-PEG-coated surface is confirmed by whole blood flow experiments where no thrombi and less serum protein adsorption are observed when compared with bare glass, polyethylene (PE), and polyethylene terephthalate (PET) surfaces. Furthermore, unlike bare PE films, less fibrosis and inflammation are observed when the PP-PEG-coated PE film is implanted into subcutaneous pockets of mice groin areas. The cell-repellent property of PP-PEG is also verified via patterning of mammalian cells, such as fibroblasts and hippocampal neurons. These results show that our PP-PEG film, generated by the CCP-CVD method, is a biocompatible material that can be considered for broad applications in biomedical and functional materials fields.

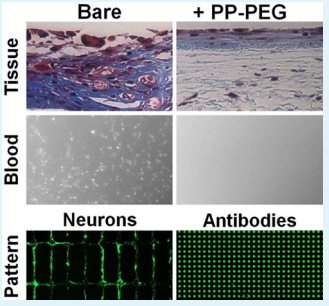

KEYWORDS: *plasma-polymerized poly(ethylene glycol) (PP-PEG), plasma-enhanced chemical vapor deposition (PECVD), biocompatibility, nonfouling, cell patterning*

INTRODUCTION

Biocompatible materials have been widely used in many fields, such as medicine, medical devices, tissue engineering, and materials science. For in vivo and in vitro applications, a low immune response in tissue (histocompatibility) and good blood compatibility (hemocompatibility) are the most important properties for biocompatible materials.[1−3] Poly(ethylene glycol) (PEG) polymer is a well-known coating material that acts as an effective repellent against proteins and cell adsorption, offering sufficient biocompatibility. As such, the Food and Drug Administration (FDA) has approved the PEG polymer for human use. It has been a great challenge, however, to coat substrates with PEG polymer because the PEG molecules form a viscous liquid or wax at room temperature and dissolve easily in an aqueous environment. To resolve this issue, various PEG coating techniques, including graft polymerization,[4] self-assembled monolayer (SAM) formation,[5] and plasma polymerization,[6] have been developed. In particular, special attention has been focused on plasma-enhanced chemical vapor deposition (PECVD) because of its high reproducibility, chemical stability, scalability, uniformity, and adaptability to various film depositions.[7] However, the low vapor pressure of PEG polymer precursors makes the PECVD method far from being used for common application for PEG film generation.[8−11] To overcome this shortcoming, ethylene glycol (EG)-based ether molecules (glymes)[12−29] and lower molecular weight PEG polymer (PEG200)[6] that have higher vapor pressures than PEG polymers have been used as precursors, which showed marginal blood compatibility with the lack of evaluation of tissue compatibility.

Here, to address both hemo- and histocompatibility issues while keeping the benefits of PECVD, we generated a novel PEG-like film using, among other PECVD methods, the capacitively coupled plasma (CCP)-CVD method that generates large and uniform plasma, and using nontoxic PEG200 precursor that has high enough vapor pressure for

Received: October 4, 2012
Accepted: January 2, 2013
Published: January 2, 2013

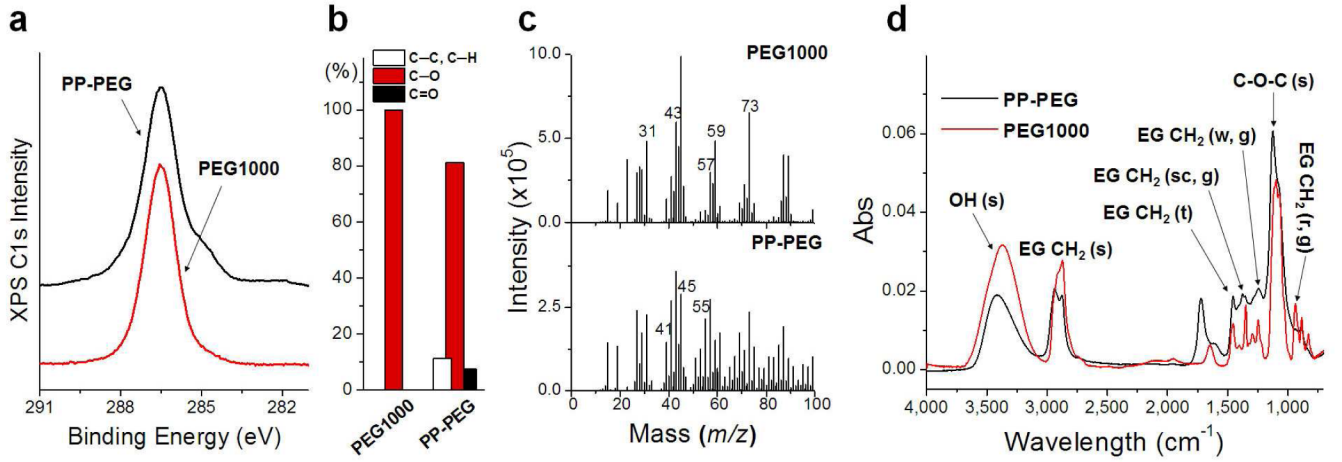

Figure 1. Characterization of chemical similarity between PEG1000 polymer (average M_w: 1000 Da) and PP-PEG. (a) XPS C 1s spectra of PEG1000 and PP-PEG film. (b) Peak fitting the XPS C 1s peak of PP-PEG in (a) revealed C—C/C—H and C═O bond composition. (c) TOF-SIMS spectra of PEG1000 and PP-PEG film. PEG-related peaks (CH_3O^+, m/z 31; C_2HO^+, m/z 41; $C_2H_3O^+$, m/z 43; $C_2H_5O^+$, m/z 45; $C_3H_3O^+$, m/z 55; $C_3H_5O^+$, m/z 57; $C_3H_7O^+$, m/z 59; $C_3H_5O_2^+$, m/z 73) appeared from both PEG1000 and PP-PEG samples. (d) FT-IR spectra of the PEG1000 and PP-PEG with superimposed peaks corresponding to streching (s), wagging (w), twisting (t), rocking (r), and scissoring (sc) vibrational modes originating from the ethylene glycol (EG) unit. (g) stands for gauche form.

the PECVD procedure. We thoroughly demonstrate a "multi-parameter" assessment of superior biocompatibility,[30] with chemical similarity to intact PEG polymers, of the newly generated plasma-polymerized PEG (PP-PEG) films on various substrates, for example, glass, indium tin oxide (ITO), polyethylene (PE), and polyethylene terephthalate (PET).

RESULTS AND DISCUSSION

Chemical and Physical Characterization of PP-PEG. In PECVD methods, the lower the radio frequency (RF) power for plasma evaporation, the better the chemical identity of the precursor and the target materials is preserved. We thus employed 2 W of RF power for the plasma evaporation of PEG200, much lower than the one reported by Kumar et al. where 50 W of plasma power was used at the expense of chemical similarity to native PEG polymer and blood/tissue compatibility.[6] Since the lower plasma power usually yields low adhesiveness of the deposited materials, it is of importance to evaluate the adhesiveness of PP-PEG film generated with 2 W plasma power. When we tested the durability of PP-PEG in water and ethanol, the film showed superior stability that enabled us to proceed for further evaluation (Figure S1 in Supporting Information). Furthermore, the PP-PEG thin film proved to be exceptionally flat (roughness ~ 0.247 nm) and hydrophilic (contact angle ~ 40°) (Figures S2 and S3 in Supporting Information), which are all prerequisite characteristics for in vitro and in vivo biocompatibility.

We then characterized the chemical similarity between the newly fabricated PP-PEG and the normal PEG1000 polymer (average M_r = 1000) using X-ray photoelectron spectroscopy (XPS), time-of-flight secondary ion mass spectrometry (TOF-SIMS), and Fourier transform infrared (FT-IR) absorption spectroscopy. In XPS, the binding energy of carbon element (C 1s) for both PP-PEG and PEG1000 was essentially identical with the major chemical shift at 286.5 eV for the C—O bond of CH_3CH_2O unit, indicating that both polymers have similar chemical environments (Figure 1a). When we evaluated the newly generated chemical bonds, we found that C—C/C—H (285.0 eV) and C═O (287.8 eV) comprised 11% and 7% of XPS C 1s intensity, respectively (Figure 1b). On the basis of these XPS results, we were able to conclude that our PP-PEG surface has a PEG-like surface and that the quality of this surface is comparable to that of the plasma-deposited tetraglyme surface fabricated by Ratner's group (see Figure S4 in Supporting Information).[16] In the TOF-SIMS experiment, although the distribution profile and the intensities of the peaks are slightly different, PP-PEG and PEG1000 exhibited similar mass peaks corresponding to PEG-related fragment molecules (Figure 1c). When we compared FT-IR spectra of PP-PEG and PEG1000, the peaks for stretching and bending vibrational modes of the ethylene glycol unit were in good agreement with each other (Figure 1d).

Blood Compatibility Test. To demonstrate the in vitro biocompatibility, the blood biocompatibility of the newly generated plasma-polymerized PEG (PP-PEG) film was investigated by an in vitro blood test. Since the circulation of blood along the vessel plays important and diverse roles in the delivery of nutrients and oxygen, immune reactions, and blood coagulation (thrombosis),[31] we developed an in vitro blood circulation system that is similar to the in vitro catheterization model (or disturbed blood flow model) to measure thrombus deposition on catheters (Figure 2a,b).[30] We prepared glass, low density polyethylene (LDPE), and PET, each of which was either PP-PEG-coated or uncoated, and put it into the blood in circulation for 1 h. As expected, all three uncoated surfaces showed a thrombus adhesion as shown in the scanning electron microscope (SEM) images in Figure 2c, upper panels, although the amount of clotted blood on each surface varied. Surprisingly, none of the three PP-PEG-coated surfaces resulted in thrombus adhesion (Figure 2c, lower panels). Since a thrombus is initiated via platelets aggregation in blood plasmas, i.e., whole blood without cells,[32,33] we confirmed the antiadhesive effect of the PP-PEG layer using human blood plasma. Indeed, no platelet adhesion was observed on PP-PEG-coated glass, whereas a tremendous amount of platelet aggregation was visible on bare glass (Figure 3). Note that the aggregation was accelerated when the glass surface was pretreated with 1% human plasma, showing plasma-dependent platelet aggregation. Thus, we can conclude that the PP-PEG

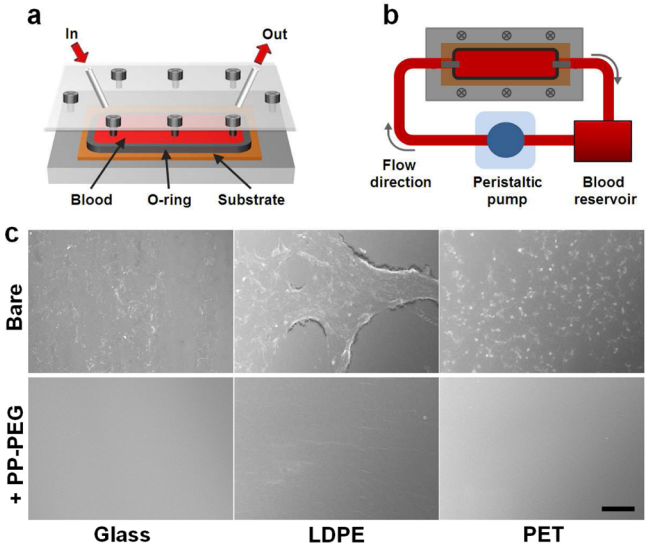

Figure 2. Blood compatibility of PP-PEG films coated on various substrates. (a) Schematic illustration of the sample holder for the blood circulation system shown in (b). (c) SEM images of bare and PP-PEG-coated glass, LDPE, and PET substrates after 4 h of exposure to the blood flow. Scale bar = 20 μm.

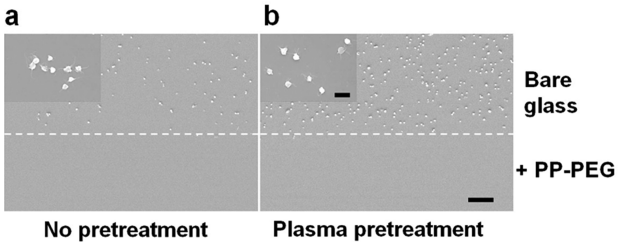

Figure 3. (a) SEM images showing no platelet aggregation on PP-PEG-layered glass surface upon exposure to blood plasma. Pretreatment with 1% plasma accelerated the aggregation of platelets on bare glass surface (b). Scale bar = 2 μm for high resolution insets, 25 μm for low resolution images.

film effectively deters the adsorption of plasma proteins by avoiding platelet adhesion on the coated surface.

Next, we tested adsorption of blood proteins on the PP-PEG film using human serum, i.e., whole blood without cells and clotting factors. The surface of serum-treated ITO slides with or without PP-PEG deposition was analyzed using matrix-assisted laser desorption/ionization time-of-flight mass spectrometry (MALDI-TOF MS), XPS, and TOF-SIMS. As shown in the MALDI-TOF spectra (Figure 4a), protein adsorption was undetectable on the PP-PEG-coated ITO slides, whereas a large amount of blood proteins, such as connective tissue-activating peptide III (CTAP III, M_r = 9278)[34] and apolipoprotein CII (32−90) (Apo-CII, M_r = 6627),[35] could be observed on the bare ITO slides. The insufficient quantitative analysis of MALDI-TOF was complemented by XPS and TOF-SIMS, which showed that the PP-PEG films exposed to human serum contains a negligible amount of serum proteins; the intensity of the nitrogen (N) 1s spectra, direct evidence of protein adsorption, was reduced from 2.1% to 0.4% (in XPS, Figure 4b), and most of the peak intensities of amino acids decreased (in TOF-SIMS, Figure 4c) in the case of the PP-PEG-coated surface. In addition, little difference was observed between 4 and 24 h incubation samples, suggesting that the adsorption of

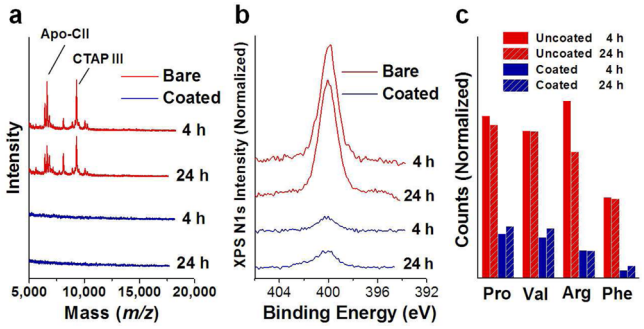

Figure 4. Human serum adsorption profile of bare and PP-PEG-coated ITO surfaces. (a) MALDI-TOF MS shows blood protein peaks only on bare surface. (b) XPS spectra exhibit a dramatic decrease in peak intensity of amino acid-derived nitrogen 1s in the case of PP-PEG-deposited ITO. (c) Normalized TOF-SIMS counts show reduced amino acid peaks on PP-PEG coated ITO surfaces, regardless of incubation time (m/z = 68.05, $C_4H_6N^+$, proline; m/z = 72.08, $C_4H_{10}N^+$, valine; m/z = 73.06, $C_2H_7N_3^+$, arginine; m/z = 120.08, $C_8H_{10}N^+$, phenylalanine).

serum proteins was completed within four hours and no further adsorption ensued.

Tissue Compatibility Test. To investigate in vivo biocompatibility, i.e., histocompatibility, of the PP-PEG films, we implanted polyethylene (PE) films with and without PP-PEG coating into the subcutaneous pockets of both groin areas of C57BL/6J mice aged 10−12 weeks. We then removed the films from the subcutaneous pockets after one and four weeks of implantation and examined severity and surface morphology. In a systematic severity test of four weeks of implantation, the bare PE film showed significant levels of adhesions in contrast to PP-PEG-treated film (Table 1).[35] By the naked eye, the bare and

Table 1. Severity of the Adhesions According to Lamination with or without PP-PEG Coating

group	time (week)	grade (number of animals)
bare PE	1	1 (5)
	4	3 (4), 4 (1)
PP-PEG PE	1	0 (2), 1 (3)
	4	0 (1), 1 (4)

PP-PEG film could be easily distinguished, with the latter being much more clean (Figure 5, top). When we examined the tissue from subcutaneous pockets that had been contacting with the films using hematoxylin and eosin staining to evaluate inflammatory changes,[36,37] the bare film caused greater degree of inflammation (Figure 5, middle). Masson's trichrome staining was also performed to demonstrate the degree of fibrous proliferation[26] induced by the films with or without the PP-PEG coating. As expected, compared with the bare film, the PP-PEG film was associated with a dramatic decrease in fibrous proliferation (Figure 5, bottom). The exceptionally low toxicity of the PP-PEG surface was also verified using WST-1 assay kit (Roche, Mannheim, Germany). In this case, the viability of the cells cultured on a PP-PEG-coated dish was similar to that of the cells cultured on a conventional culture dish (Figure S5 in Supporting Information). Taken together, the PP-PEG showed superior biocompatibility and minimum toxicity.

Use of PP-PEG in Cell and Protein Micropatterning. For both in vivo and in vitro applications and for biomedical applications in particular, PEG-like thin films must be uniformly

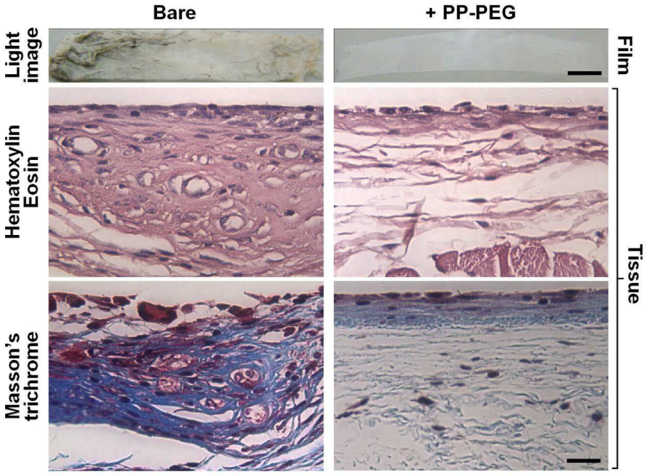

Figure 5. Inflammation and fibrous propagation after four weeks of implantation of bare and PP-PEG-coated PE films in mice subcutaneous pockets. Light microscopy of the removed films (top), histological examination of contacting tissue using hematoxylin and eosin staining for the inflammation assessment (middle), and Masson's trichrome staining for the fibrous propagation assay (bottom). Scale bar = 5 mm for light images, 20 μm for stained images.

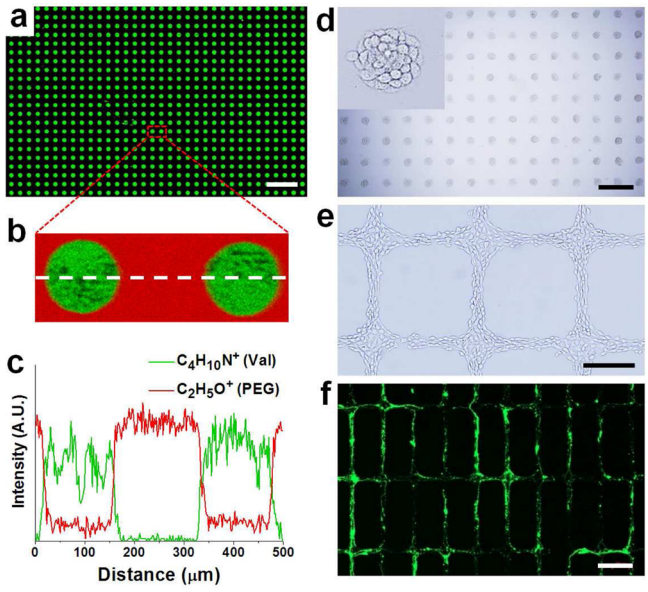

Figure 6. Cell culture and protein adsorption demonstrate the uniformity of CCP-CVD of PP-PEG and PP-amine. (a) Fluorescence image of FITC-tagged IgG protein immobilized on the PP-amine patterned surface. (b) TOF-SIMS image of selected area. Signals from PEG ($C_2H_5O^+$) and IgG ($C_4H_{10}N^+$, valine) were pseudocolored to red and green, respectively. (c) Line profiles of the dashed line in (b). (d) Optical image of NIH-3T3 fibroblast cells grown on patterned surfaces for 1 d. Cells in a single PP-amine dot pattern are magnified in the inset. (e) Optical images of the fibroblasts on PP-PEG-patterned PDK-glass. (f) Primary culture of hippocampal neurons on PP-PEG-patterned PDK-glass. For clarity, green fluorescence protein (GFP) was transfected. Scale bars = 1.0 (a), 0.5 (d), 0.25 (e), and 0.2 mm (f).

deposited or patterned over a large area. To test the uniformity of deposition, the PP-PEG was deposited over a large area of glass slide (10 mm ×10 mm), followed by plasma-polymerized amine (PP-amine) deposition through a patterned metal shadow mask.[38−40] When we treated the surface with fluorescein isothiocyanate (FITC)-tagged IgG, we could observe a clear discrimination of fluorescence (Figure 6a), which was verified with TOF-SIMS where no signs of proteins were observed in the PP-PEG-coated areas (Figure 6b,c). We then cultured NIH 3T3 fibroblasts on the patterned glass. As seen in Figure 6d, all cells adhered to the PP-amine layer while avoiding the PP-PEG layer. Next, to evaluate the versatility of the PP-PEG patterning, we first treated glass slides with poly-D-lysine (PDK), a well-known in vitro cell adhesion molecule, and generated island patterns of PP-PEG (Figure S6 in Supporting Information). When we cultured the fibroblasts and hippocampal neurons on the PDK- and PP-PEG-patterned glass, the cells grew within the exposed PDK layer (Figure 6e,f and Figure S7 in Supporting Information). These results confirm that the PP-PEG can be uniformly coated over a large area and can be easily patterned for the use in long-term micropatterning of cells and protein microarrays.

PEG patterning is one of the most exploited "nonfouling" surfaces for patterning proteins and cells. For example, Grainger and co-workers[29] made a photoresist pattern on the NHS-terminated PEG (M_r = 3400, OptiChem) surface using photolithography and partially methoxylated the developed NHS layer to make a PEG-like surface for blocking cells and proteins. The NHS-PEG, however, uses silane-based chemistry for its solution-based coating, which limits the substrates to glass-based materials. By contrast, not only can the PP-PEG film be deposited on a variety of substrates including, but not limited to, glass, ITO, PE, PET, and even PDK (see Figure S6 in Supporting Information), but also the film can be directly used as a nonfouling substrate without any additional chemical treatment. Chang and Sretavan[19] employed plasma polymerized diglyme in conjunction with photolithography to produce a polylysine pattern for neuron culture. Unlike ours, they generated the photoresist pattern first, followed by O_2 plasma and polylysine treatment. The experiment has clearly demonstrated that polylysine can adsorb to the PEG-like film and produce as small as 1 μm lanes. We, on the contrary, generated the PDK layer first followed by PP-PEG deposition and removed an additional step such as O_2 plasma treatment, yielding reduced resolution that can be easily restored by the reversal of the procedure for PDK and PP-PEG deposition.

CONCLUSION

In this paper, we thoroughly demonstrated hemo- and histocompatibility of a novel PP-PEG film generated on a variety of substrates by merging the advantages of the CCP-CVD method and the low molecular weight PEG200 precursor that has higher vapor pressure. By applying low plasma power, we were able to secure the chemical identity of PEG200 precursor and thus minimize potential toxicity originating from the reorganized chemical bonds. The PP-PEG film effectively inhibited thrombus deposition when exposed to circulating whole blood and is highly resistant to fouling by platelet aggregation, serum proteins adsorption, and cellular adhesion. Importantly, when implanted in mouse subcutaneous tissue, the PP-PEG-coated film showed superior histocompatibility, as exhibited by minimal tissue adhesion, inflammation, and fibrous proliferation. Because a judicious balance between efficacy and safety must always be maintained, the practical significance of emerging biomedical devices centers mostly on whether the manufactured devices can be easily generated and safely applied to biomedical conditions without toxicity. Our results suggest

that our PP-PEG film would maintain this balance and could therefore be extensively applied to various biomedical devices to improve biocompatibility.

EXPERIMENTAL SECTION

PP-PEG Deposition. PEG200 polymer (average M_r = 200 Da; Sigma-Aldrich, St. Louis, USA) was placed into a stainless steel bubbler and heated at 115 °C until vaporized. All delivery lines were kept at 140 °C. The substrate was put on the substrate holder in the deposition chamber, and the pressure was kept below a few mTorr using a rotary vane pump. The flow rate of argon gas was kept at 1 SCCM (SCCM denotes cubic centimeters per minute at STP) using a mass flow controller (MFC). The argon gas flowed into the bubbler that contained the PEG 200 precursor and bubbled through it. The gas mixture flowed into the deposition chamber through the shower ring. Capacitively coupled plasma (CCP) using a power of 2 W was generated above the shower ring, which was directly connected to a 13.56 MHz radio frequency (RF) generator through a matching network. During deposition, the pressure in the chamber was kept at 100 mTorr using a throttle valve, and the deposition time was 30 min. For surface cleaning, all substrates were sonicated with trichloroethylene, acetone, and methanol for 5 min, respectively. The substrates were subsequently rinsed with deionized water and dried using nitrogen gas.

In Vitro Whole Blood Interaction Test. First, the PP-PEG films were deposited on glass slides, LDPE films, and PET films. Human whole blood was obtained from healthy human volunteers, and the fresh blood was used within 7 days of donation. For anticoagulation treatment, whole blood and acid citrate dextrose (ACD, Sigma-Aldrich, St. Louis, USA) solution were mixed in a ratio of 9:1 (v/v). Whole blood, which was maintained at 37 °C in a warm bath, was connected to a blood flow device with a 3.2 mm ID Tygon tube. A peristaltic pump was used to induce blood flow at approximately 70 mL/min for 1 h. After exposure to blood, all samples were washed three times with PBS buffer and fixed using 2% (w/v) glutaraldehyde. Samples were sputter-coated with gold for SEM analysis.

Platelet Adhesion. Human platelets were obtained from healthy human donors by centrifugation. Briefly, peripheral blood was drawn into a syringe containing EDTA. Platelet rich plasma (PRP) was obtained by centrifuging the blood at 200 × *g* for 15 min, and the platelet pellets were isolated by a second centrifugation at 1000 × *g* for 20 min. The isolated platelets were suspended in platelet suspension buffer (PSB) with a concentration of 1.0×10^8 platelets/mL. The PSB contained 137 mM NaCl, 2.7 mM KCl, 0.4 mM Na_2HPO_4, 5.5 mM dextrose, 10 mM HEPES, 4 mg/mL bovine serum albumin, 0.1 U/mL apyrase, 2.5 mM $CaCl_2$, and 1.0 mM $MgCl_2$. Bare and PP-PEG-coated glass slides were put into 6-well plates and preadsorbed with 1% BSA to prevent platelet activation by the polystyrene wells of the 6-well plates. The samples were incubated for one hour at 37 °C and rinsed three times with PBS. Next, the slides were incubated in PBS or plasma (1% in PBS) for 30 min at 37 °C and washed three times with PBS. Platelets were then added to each slide for 2 h at 37 °C in a horizontal shaker at 40 rpm. Thereafter, the slides were rinsed three times with PBS to remove any remaining platelets. For platelet fixation, all samples were fixed using 2% (w/v) glutaraldehyde and then gradually dehydrated with a series of ethanol solutions of increasing concentration (50, 60, 70, 80, 90, and 100%); the samples were immersed in each solution for 10 min. SEM was used to observe adherent platelets and their morphology.

Human Serum Adsorption and MALDI-TOF, XPS, and TOF-SIMS Measurements. Bare and PP-PEG-coated ITO glass slides were immersed in human serum for 4 or 24 h. After immersion, all substrates were washed twice with PBS buffer and then rinsed using deionized water. Sinapinic acid (10 mg/mL, Sigma-Aldrich) as a MALDI matrix was spotted and air-dried on the sample surface for MALDI-TOF analysis. In the XPS spectra, the carbon (C) 1s binding energy of C—C or C—H bonds was shifted to 285.0 eV to correct for the surface charging effect. For quantitative analysis, the Shirley Method for background removal was used in conjunction with a least-squares fitting algorithm employing full Voigt functions. TOF-SIMS measurements were taken using a TOF-SIMS V instrument (ION-TOF GmbH). Bi_3^+ primary ions at 25 kV and a repetition rate of 5 kHz in the low-current bunched mode were used to obtain positive spectra. A positive spectrum was obtained for an area of 500 × 500 μm^2 with a 100 μs cycle time, and the PIDD (primary ion dose density) for analysis was 1.0×10^{12} ions/cm^2 to ensure static SIMS conditions. For mass calibration, the CH_3^+, $C_2H_3^+$, and $C_3H_5^+$ peaks were used for positive spectra.

Analysis of the In Vivo Biocompatibility of the PP-PEG Film. To demonstrate the in vivo biocompatibility of the PP-PEG film, we implanted polyethylene (PE) films with and without PP-PEG coating into the subcutaneous pockets of both groin areas of C57BL/6J mice aged 10 to 12 weeks. Under general anesthesia, which was achieved intramuscularly with 30−45 mg/kg of ketamine hydrochloride and 5−10 mg/kg of xylazine hydrochloride, the groin areas of the mice were shaved and sterilized with an alcohol swab. Subsequently, skin incisions were made, and blunt dissection was performed to make the subcutaneous pockets. Bare or PP-PEG-coated films were inserted into each subcutaneous pocket, and the skin incisions were repaired with interrupted sutures. All experiments were performed on 5 mice for each group. Under the same anesthesia, the mice were euthanized 1 and 4 weeks postoperatively, and the samples containing skin, film, and underlying serosa were excised, fixed with 4% formalin, and embedded in paraffin after the sacrifice of the animals. We stained the sections with hematoxylin and eosin to evaluate the inflammatory changes in each subcutaneous pocket. Additionally, Masson's trichrome staining was performed to demonstrate the degree of fibrous proliferation induced by the films with or without coating with PP-PEG.

Measurements of the In Vivo Severity of Adhesion. The severity of the adhesions was semiquantitatively evaluated at 1 and 4 weeks postoperatively by graded scores, as previously described: 0 = no adhesion, 1 = filmy adhesion easily separable with blunt dissection, 2 = mild to moderate adhesion with a freely dissectible plane, 3 = moderate to dense adhesion with difficult dissection, and 4 = nondissectible plane.[36] The severity of the adhesions was analyzed using the Mann−Whitney *U*-test. Statistical significance was determined at a p value of 0.05 (see Table 1).

In Vitro Toxicity Measurement. The in vitro toxicity of the PP-PEG film was measured using a WST-1 kit (Roche, Mannheim, Germany). Rat intestinal (IEC-18) cells were cultured on a PP-PEG surface and a normal culture plate for one day each. Cells of various concentrations in the wells (1 mL) were transferred to a 96-well plate. Each well contained 1 mL of medium to which 100 μL of WST-1 reagent was added. The plates were then incubated at 37 °C for 4 h. Samples were then shaken for 1 min, and the absorbance at 450 nm was measured with an ELISA reader.

Protein Immobilization and Cell Adhesion. Before protein immobilization, 1-ethyl-3-[3-dimethylaminopropyl] carbodiimide hydrochloride (EDC, 1 mg/mL, Pierce Biotechnology, Rockford, IL, USA) was dropped onto a patterned surface. After 10 min, the EDC solution was removed from the patterned glass slide with a pipet, and FITC-tagged IgG (100 μg/mL, Invitrogen) was then dropped onto the surface of the slide, after which the patterned slide was washed with phosphate-buffered saline (PBS, pH 7.4) and dried at room temperature. The amount of protein immobilized on the slide was then measured using a fluorescence laser scanner. The excitation and emission wavelengths were 488 and 520 nm, respectively. NIH 3T3 fibroblast cells were cultured on the patterned slide in an incubator that was maintained at 37 °C with 5% CO_2. After incubation for 1 day, the cell-cultured slides were washed twice with PBS. Optical images were taken using an optical microscope (Olympus IX-71, Japan).

Neuronal Cell Culture on PP-PEG/PDK Patterned Glass. The rinsed glass slide (75 × 25 × 1 mm, Marienfeld, Germany) was treated with poly-D-lysine (PDK) solution (500 μg/mL in 0.1 M borate buffer, pH 8.5) overnight, washed, dried, coated with photoresist AZ 5214 E (Clariant), UV-irradiated under a film mask, developed with AZ 300 MIF (AZ Electronic Materials), and deposited with PP-PEG. After removal of PR, the patterned glass was used for primary neuron culture. Hippocampus dissected from E18 rat embryos was rinsed with

HBSS followed by incubation with papain and DNase with 60 rpm for 30 min at 37 °C. After sequential rinsing with HBSS containing 10% and 5% FBS, individual single cells were mechanically isolated by trituration 10 times in 2 mL of HBSS containing DNase with a silanized Pasteur pipet. The cells were diluted to a density of 2×10^5 cells/mL with plating media containing MEM supplemented with 0.6% (w/v) glucose, 10 mM sodium pyruvate, 1 mg/mL FBS, and 1% penicillin-streptomycin. The cell-media solution was plated on the PP-PEG patterned PDK-coated glasses and placed in a Petri dish. The cell culture media was exchanged with B27-supplemented neurobasal media containing 2 mM glutamax after 3 h, and the cultures were maintained in an incubator at 37 °C with 5% CO_2.

■ ASSOCIATED CONTENT

Supporting Information

Supplementary Figures S1−S7 and Table S1. This material is available free of charge via the Internet at http://pubs.acs.org.

■ AUTHOR INFORMATION

Corresponding Author

*E-mail addresses: steph25@snu.ac.kr (J.H.K), tdchung@snu.ac.kr (T.D.C), tglee@kriss.re.kr (T.G.L).

Author Contributions

▽These authors contributed equally.

Notes

The authors declare no competing financial interest.

■ ACKNOWLEDGMENTS

We thank healthy volunteers who provided blood samples and expedited hemocompatibility experiments. This work was supported in part by the Pioneer Research Program (2012-0009541), the Bio-Signal Analysis Technology Innovation Program (2011-0027718), the Converging Research Center for Mass Spectrometric Diagnosis (2011K000887) of the MEST/NRF, the MEST/NRF fund (2012011289), and the Development of Characterization Techniques for Nanomaterials Safety Project of KRCF.

■ ABBREVIATIONS

XPS, X-ray photoelectron spectroscopy; TOF-SIMS, time-of-flight secondary ion mass spectrometry; PP-PEG, plasma-polymerized poly(ethylene glycol); PECVD, plasma-enhanced chemical vapor deposition; CCP-CVD, capacitively coupled chemical vapor deposition; PE, polyethylene; PET, polyethylene terephthalate; ITO, indium tin oxide

■ REFERENCES

(1) Goddard, J. M.; Hotchkiss, J. H. *Prog. Polym. Sci.* **2007**, *32*, 698.
(2) Ratner, B. D. *Biomaterials* **2007**, *28*, 5144.
(3) Williams, D. F. *Biomaterials* **2008**, *29*, 2941.
(4) Delamarche, E.; Donzel, C.; Kamounah, F. S.; Wolf, H.; Geissler, M.; Stutz, R.; Schmidt-Winkel, P.; Michel, B.; Mathieu, H. J.; Schaumburg, K. *Langmuir* **2003**, *19*, 8749.
(5) Veiseh, M.; Zareie, M. H.; Zhang, M. Q. *Langmuir* **2002**, *18*, 6671.
(6) Kumar, D. S.; Fujioka, M.; Asano, K.; Shoji, A.; Jayakrishnan, A.; Yoshida, Y. *J. Mater. Sci.: Mater. Med.* **2007**, *18*, 1831.
(7) Ozaydin-Ince, G.; Coclite, A. M.; Gleason, K. K. *Rep. Prog. Phys.* **2012**, *75*, 016501.
(8) Kampfrath, G.; Hintsche, R. *Anal. Lett.* **1989**, *22*, 2423.
(9) Inagaki, N. *Plasma Surface Modification and Plasma Polymerization*; CRC Press: 1996.
(10) Biederman, H. *Plasma polymer films*; Imperial College Press: 2004.
(11) Choi, C.; Il Kim, S.; Lee, S.; Jung, D.; In, K.; Park, H. *J. Korean Phys. Soc.* **2008**, *53*, 1475.
(12) Lopez, G. P.; Ratner, B. D.; Tidwell, C. D.; Haycox, C. L.; Rapoza, R. J.; Horbett, T. A. *J. Biomed. Mater. Res.* **1992**, *26*, 415.
(13) Beyer, D.; Knoll, W.; Ringsdorf, H.; Wang, J. H.; Timmons, R. B.; Sluka, P. *J. Biomed. Mater. Res.* **1997**, *36*, 181.
(14) Shen, M. C.; Martinson, L.; Wagner, M. S.; Castner, D. G.; Ratner, B. D.; Horbett, T. A. *J. Biomater. Sci., Polym. Ed.* **2002**, *13*, 367.
(15) Zhang, Z.; Menges, B.; Timmons, R. B.; Knoll, W.; Forch, R. *Langmuir* **2003**, *19*, 4765.
(16) Johnston, E. E.; Bryers, J. D.; Ratner, B. D. *Langmuir* **2005**, *21*, 870.
(17) Bretagnol, F.; Valsesia, A.; Sasaki, T.; Ceccone, G.; Colpo, P.; Rossi, F. *Adv. Mater.* **2007**, *19*, 1947.
(18) Muir, B. W.; Tarasova, A.; Gengenbach, T. R.; Menzies, D. J.; Meagher, L.; Rovere, F.; Fairbrother, A.; McLean, K. M.; Hartley, P. G. *Langmuir* **2008**, *24*, 3828.
(19) Chang, W. C.; Sretavan, D. W. *Langmuir* **2008**, *24*, 13048.
(20) Salim, M.; Mishra, G.; Fowler, G. J. S.; O'Sullivan, B.; Wright, P. C.; McArthur, S. L. *Lab Chip* **2007**, *7*, 523.
(21) Salim, M.; Wright, P. C.; McArthur, S. L. *Electrophoresis* **2009**, *30*, 1877.
(22) Mishra, G.; Easton, C. D.; McArthur, S. L. *Langmuir* **2010**, *26*, 3720.
(23) Bretagnol, F.; Lejeune, M.; Papadopoulou-Bouraoui, A.; Hasiwa, M.; Rauscher, H.; Ceccone, G.; Colpo, P.; Rossi, F. *Acta Biomater.* **2006**, *2*, 165.
(24) Bretagnol, F.; Ceriotti, L.; Lejeune, M.; Papadopoulou-Bouraoui, A.; Hasiwa, M.; Gilliland, D.; Ceccone, G.; Colpo, P.; Rossi, F. *Plasma Process. Polym.* **2006**, *3*, 30.
(25) Bretagnol, F.; Valsesia, A.; Ceccone, G.; Colpo, P.; Gilliland, D.; Ceriotti, L.; Hasiwa, M.; Rossi, F. *Plasma Process. Polym.* **2006**, *3*, 443.
(26) Sardella, E.; Gristina, R.; Senesi, G. S.; d'Agostino, R.; Favia, P. *Plasma Process. Polym.* **2004**, *1*, 63.
(27) Favia, P.; Sardella, E.; Gristina, R.; d'Agostino, R. *Surf. Coat. Technol.* **2003**, *169−170*, 707.
(28) Sardella, E.; Gristina, R.; Ceccone, G.; Gilliland, D.; Papadopoulou-Bouraoui, A.; Rossi, F.; Senesi, G. S.; Detomaso, L.; Favia, P.; d'Agostino, R. *Surf. Coat. Technol.* **2005**, *200*, 51.
(29) Takahashi, H.; Emoto, K.; Dubey, M.; Castner, D. G.; Grainger, D. W. *Adv. Funct. Mater.* **2008**, *18*, 2079.
(30) Cao, L.; Chang, M.; Lee, C. Y.; Castner, D. G.; Sukavaneshvar, S.; Ratner, B. D.; Horbett, T. A. *J. Biomed. Mater. Res. A* **2007**, *81A*, 827.
(31) Harker, L. A.; Slichter, S. J. *Thromb. Diath. Haemorrh.* **1974**, *31*, 188.
(32) Keogh, J. R.; Eaton, J. W. *J. Lab. Clin. Med.* **1994**, *124*, 537.
(33) Subramanian, A.; Sarkar, S.; Woollam, J. A.; Nosal, W. H. *Biomed. Sci. Instrum.* **2004**, *40*, 1.
(34) Tiss, A.; Smith, C.; Menon, U.; Jacobs, I.; Timms, J. F.; Cramer, R. *Proteomics* **2010**, *10*, 3388.
(35) Tiss, A.; Smith, C.; Menon, U.; Jacobs, I.; Timms, J. F.; Cramer, R. Presented at 57th ASMS Conference on Mass Spectrometry, Philadelphia, PA, USA, 2009.
(36) Kim, J. H.; Jeong, S. Y.; Jung, M. H.; Hwang, J. M. *Brit. J. Ophthalmol.* **2004**, *88*, 1450.
(37) Kim, M. S.; Ahn, H. H.; Shin, Y. N.; Cho, M. H.; Khang, G.; Lee, H. B. *Biomaterials* **2007**, *28*, 5137.
(38) Mutlu, S.; Saber, R.; Kocum, C.; Piskin, E. *Anal. Lett.* **1999**, *32*, 317.
(39) Kim, J.; Park, H.; Jung, D.; Kim, S. *Anal. Biochem.* **2003**, *313*, 41.
(40) Kim, J.; Shon, H. K.; Jung, D.; Moon, D. W.; Han, S. Y.; Lee, T. G. *Anal. Chem.* **2005**, *77*, 4137.